Photoemission study of reactive rare-earth/semiconductor interfaces: Tm/GaAs(110) and Yb/GaAs(110)

M. Prietsch, C. Laubschat, M. Domke, and G. Kaindl
Institut für Atom- und Festkörperphysik, Freie Universität Berlin, Arnimallee 14, D-1000 Berlin 33, Germany
(Received 24 February 1987; revised manuscript received 29 February 1988)

The behavior of interfaces formed by growing thin Tm and Yb films on *p*- and *n*-type GaAs(110) substrates at room temperature was investigated by photoemission from As 3*d*, Ga 3*d*, and metal 4*f* core levels. At metal coverages $\Theta < 1$ Å, the core-level binding energies of substrate atoms are found to be shifted to higher and lower values, respectively, for *p*- and *n*-type GaAs; this observation is interpreted as a consequence of band bending due to defect states. In addition, photoemission signals from chemically reacted products at the interface are observed, which grow in intensity with metal coverage. In the coverage range $2 < \Theta < 2.8$ Å for Tm and $2.5 < \Theta < 5.6$ Å for Yb, a further change in band bending occurs, as reflected in additional shifts of all core levels towards lower binding energies. This observation, together with the strongly increasing density of states at the Fermi level around this coverage, indicates that the Schottky barrier is not established until the overlayer assumes metallic character. These observations are interpreted within the concept of metal-induced gap states defining the final Fermi-level position. From the observed variations with metal coverage of binding energies and relative intensities of photoemission signals from the reacted layer, a structure model is proposed for rare-earth/GaAs(110) interfaces that includes a separation of As and Ga atoms into As-rich and Ga-rich rare-earth compounds in the reacted zone. For Tm and Yb interfaces, respectively, the 4*f* core levels of the reaction products are found to be shifted in opposite directions from the binding energies of the elemental rare-earth metals. Employing thermochemical arguments, this behavior is explained as a consequence of the different valences of Tm (3 +) and Yb (2 +) in these compounds. At coverages around 20 Å for Tm and 30 Å for Yb, elemental rare-earth films with rough surfaces are formed, as revealed by a large surface shift of the 4*f* photoemission lines in the case of Yb and a partial surface valence transition in the case of Tm.

I. INTRODUCTION

The investigation of metal/semiconductor interfaces has attracted considerable interest in the recent past mainly due to related technological aspects.[1] Until now, however, details of the electronic structure of the interfaces, in particular the influence of interfacial gap states on the Schottky-barrier height as well as the extent of chemical reactions and interdiffusion processes, are not fully understood.[2] Essentially three major theories of the Schottky-barrier height have been formulated, including work function,[3,4] metal-induced gap states (MIGS),[5–7] and localized models.[8] Layer-resolved photoemission (PE) studies of thin metal overlayers grown on semiconductor surfaces are a powerful tool for studying these questions, since PE is capable of providing information on both the Fermi-level position as well as the electronic structure and the chemical composition of the interface.

Most previous PE work on metal/semiconductor interfaces was devoted to systems with simple metals or *d* transition metals, with emphasis on valence-band structure and semiconductor core levels. Mainly for experimental reasons, metal core levels were studied to a much smaller extent, even though they are capable of providing valuable information on band bending as well as on chemical reaction processes at the interface, and on local substrate and coordination effects. The rare-earth (RE) metals, with their highly localized, but very weakly bound 4*f* electrons, are particularly suited for such investigations, since the 4*f* electrons give rise to relatively sharp final-state 4*f* multiplets close to the Fermi level in the PE spectra. The elemental RE metals are usually in a trivalent chemical state, with the exception of the divalent metals Eu and Yb. In certain compounds and at the surface, however, valence changes, depending on local coordination and chemical environment, have been observed for several of the RE's.[9]

The RE/semiconductor interfaces investigated up to now by PE, which in most cases were formed at room temperature, are all characterized by relatively strong reaction and interdiffusion processes in the interfacial region.[10–16] The RE/GaAs(110) interfaces studied so far [with rare earths Ce,[14] Sm,[15] and Yb (Ref. 16)] were found to be composed of an As-rich chemically reacted phase near the interface and a Ga-rich phase near the surface. While the As-rich compound has an approximately constant stoichiometry, the Ga-rich compound shows an increase in RE content with coverage, as revealed by variations in the core-level binding energies (BE). This latter change in stoichiometry also explains the observed behavior of the 4*f* core levels, which exhibit continuous BE shifts with increasing coverage towards the elemental-metal values. During the growth of these interfaces, additional shifts of the As 3*d* and Ga 3*d* PE

lines of the reacted phases to lower BE's were observed at metal coverages of $\simeq 3$ Å. These shifts were interpreted in terms of a transition from a weakly reacted to a chemically stronger reacted phase at higher metal coverages.[14–16]

In the present study, similar BE shifts are also observed for PE lines from the As 3*d* and Ga 3*d* substrate core levels, and it is shown that these shifts occur at metal coverages when a strongly increasing density of states at the Fermi level in the valence-band PE spectra signals a metallization of the overlayer. The final Fermi-level position derived from the PE spectra agrees well with the value expected from current-voltage measurements. Thus, the additional shifts occurring at $\Theta \simeq 3$ Å are interpreted as due to interface metallization, leading to a change in band bending as determined by metal-induced gap states (MIGS).[5–7] These aspects of the present research have recently been reported in a letter for Tm/GaAs(110).[17] In the present paper greater details are given as well as further data on the Yb/GaAs(110) interfacial system. The adoption of such metallization-induced shifts leads also to a simplification of the chemical and structural models necessary to describe the growth of RE/GaAs(110) interfaces. From the observed variations of binding energies and intensities of core-level PE lines with metal coverage, a detailed model for the chemical structure of RE/GaAs(110) interfaces is given.

The paper is organized as follows. After a short section (Sec. II) on experimental details, the results are presented in Sec. III for the two interfaces studied. The observed band-bending behavior as a function of metal coverage is discussed in Sec. IV in connection with theoretical models for Schottky-barrier formation. In Sec. V general aspects of the chemical structure and morphology of RE/GaAs(110) interfaces are discussed. Section VI gives a summary of the present results.

II. EXPERIMENTAL DETAILS AND DATA ANALYSIS

The measurements were performed with synchrotron radiation from the Berliner Elektronenspeicherring für Synchrotronstrahlung (BESSY), using the SX700 monochromator, or with light from a He resonance lamp. The Tm/GaAs(110) spectra were obtained with a hemispherical energy analyzer in normal-emission geometry (acceptance angle $\simeq 10°$). For the Yb/GaAs(110) experiments, a double-pass cylindrical mirror analyzer (CMA), aligned at an angle of 45° with its axis relative to the surface normal, was used. The total-system resolution was $\simeq 0.15$ eV, and the reproducibility of relative BE's is estimated as ± 0.03 eV in the synchrotron-radiation measurements[18] or ± 0.01 eV in the resonance-lamp spectra. All experiments were performed at room temperature in experimental chambers with base pressures better than 10^{-10} mbar.

Clean GaAs(110) surfaces were prepared by cleaving single crystals (dimension: $4\times 5\times 10$ mm) of Zn-doped *p*-type GaAs (doping concentration: 1×10^{18} atoms/cm^3) or Si-doped *n*-type GaAs (2.8×10^{18} atoms/cm^3). Only mirrorlike cleaved surfaces were studied further. The interfaces were prepared by evaporating 99.99% pure Tm metal from a W basket, and 99.99% pure Yb metal from an electron-beam source. During evaporation, the pressure in the chamber rose briefly to $\simeq 2\times 10^{-9}$ mbar, mainly due to metal-bound hydrogen, as monitored by mass spectrometry; it fell back to base pressure within seconds after evaporation. The evaporation rates of typically 5–20 Å/min were measured with a quartz-crystal balance with an absolute accuracy of 30%, whereas the relative accuracy for consecutive evaporations of a given metal is estimated as 15%. In the following, RE coverages Θ are given in Å, where one elemental monolayer corresponds to $\Theta \simeq 2.8$ Å for Tm and $\Theta \simeq 3.2$ Å for Yb.

The As 3*d*, Ga 3*d*, Tm 4*f*, and Yb 4*f* core-level spectra were taken with synchrotron-radiation light of energies $h\nu = 83$, 60, 70, and 80 eV, respectively, in order to achieve comparable surface sensitivities, good monochromator resolution, as well as sufficiently high PE cross sections for the RE 4*f* lines relative to valence-band emission. At these photon energies, the electron mean free paths of photoelectrons from the As 3*d* and Ga 3*d* levels ($E_{\rm kin} \simeq 37$ eV) are similar to those of the RE 4*f* photoelectrons ($E_{\rm kin} = 50$–73 eV). For Tm/GaAs(110), valence-band and Ga 3*d* core-level PE spectra were also taken with He I ($h\nu = 21.2$ eV) and He II radiation ($h\nu = 40.8$ eV), respectively.

For a quantitative analysis of the spectra, least-squares fits with Gaussian lines were performed, based on the assumption that their finite widths result mostly from limited spectroscopic resolution and inhomogeneities of the samples. The As 3*d* and Ga 3*d* core levels were additionally convolved with a Lorentzian line (FWHM of 0.2 eV), in order to take lifetime broadening into account. In this way, the 3*d* core-level spectra were found to consist of doublets with spin-orbit splittings of 0.70 ± 0.02 eV (As) and 0.44 ± 0.02 eV (Ga), respectively, and an intensity ratio of 3:2.[19] The background in the spectra could be described in a satisfactory way by a straight line. The $4f^{12}$ and $4f^{11}$ final-state multiplets of divalent and trivalent Tm, respectively, were taken from the results of intermediate-coupling calculations,[20] with appropriate adjustment of the energy splitting (10% increase in the case of $4f^{11}$ and 5% decrease in the case of $4f^{12}$). The 4*f* spectrum of Yb is a doublet with a spin-orbit splitting of 1.27 eV. The intensities of the 4*f*-multiplet components at higher BE's were adjusted by assuming an exponential decrease in PE intensity with increasing BE (decay constant: $\simeq 9$ eV for Tm and $\simeq 20$ eV for Yb). In both cases, the valence-band background was approximately described by a polygon line, superimposed on an integral background, which arises mainly from inelastic scattering of photoelectrons emitted from bulk 4*f* states.[21]

III. EXPERIMENTAL RESULTS

A. Tm/GaAs(110) interface

In Fig. 1, PE spectra of the As 3*d* and Ga 3*d* core levels for various Tm coverages, as well as least-squares

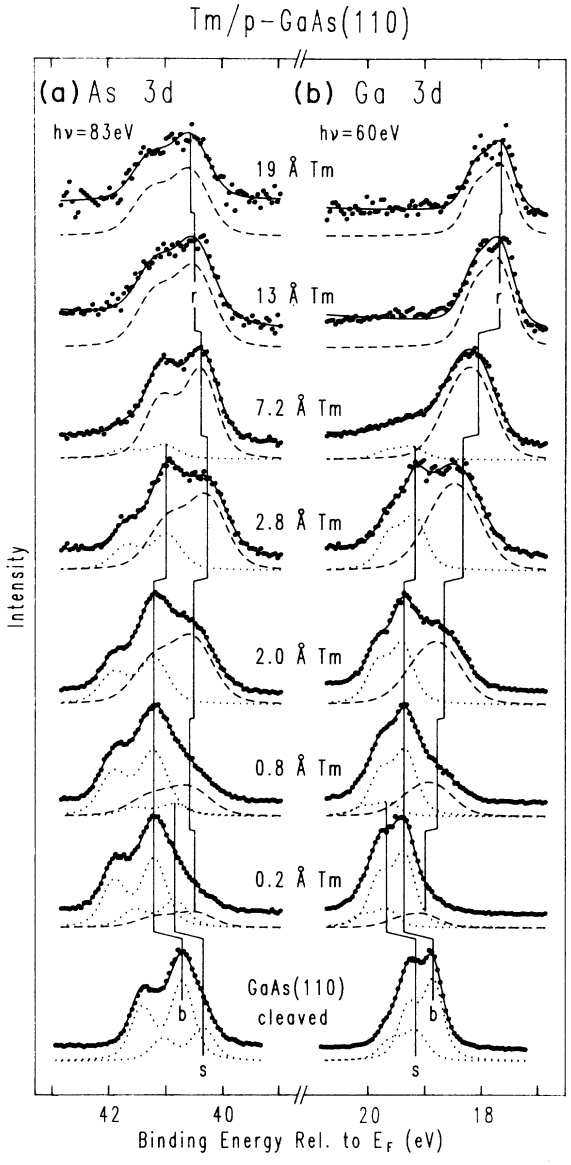

FIG. 1. Photoemission spectra of the Tm/*p*-type-GaAs(110) interface as a function of Tm coverage, with the signals from (a) As 3*d* and (b) Ga 3*d* core levels plotted separately. The solid lines through the data points represent the results of least-squares fits. The dotted subspectra originate from unreacted GaAs, while the dashed components come from the reacted overlayer. Surface and bulk contributions are denoted by *s* and *b*, respectively, and the reacted overlayer by *r*. All spectra are normalized to equal height.

fitted curves (solid lines) and individual subspectra, are shown for the Tm/*p*-type-GaAs(110) interface. The freshly cleaved semiconductor surface exhibits spin-orbit split final-state doublets, both for bulk and surface atoms. The spectra are well described by a surface core-level shift of -0.37 ± 0.03 eV in case of the As 3*d* and of $+0.31\pm0.03$ eV for the Ga 3*d* core levels, in good agreement with previously published values.[19] At a Tm coverage of 0.2 Å, a simultaneous shift of both bulk and surface PE signals by 0.5 eV to higher BE's is observed, which is caused by band bending. With increasing Tm coverage, the surface emission decreases relative to the bulk emission and finally vanishes. In addition, new spectral components at lower BE appear in both the As 3*d* and Ga 3*d* spectra, whose intensities increase with Tm coverage. These components are assigned to As or Ga atoms that have chemically reacted or alloyed with Tm. The linewidths of these reacted components are broader than those of the substrate signals, pointing to chemical or structural inhomogeneities. The relative intensities of these reacted components are approximately equal for As 3*d* and Ga 3*d*, and exceed typical surface intensities for Tm coverages higher than 0.8 Å (see Fig. 1). This shows that more than one monolayer of GaAs is affected by chemical reaction with Tm, i.e., one has to assume the formation of a reacted interface layer with a thickness of a few atomic layers containing As, Ga, and Tm atoms.

At Tm coverages between 2 and 2.8 Å, additional shifts of all spectral components to lower BE's are observed. As shown recently, the origin of these shifts lies mainly in a second band bending upon metallization of the interfacial region, which represents a transition from defect-level pinning to pinning due to metal-induced gap states.[17] Such an additional band bending will lead to identical BE shifts of the core levels in both the unreacted (substrate) and the reacted layers.[22] These aspects of the present work will be discussed in more detail in Sec. IV. At coverages exceeding 2.8 Å, the doublets from bulk substrate atoms remain at the same BE's, but their intensities decrease relative to emission from the reacted overlayer; above 8 Å, the substrate signals are too faint for identification. It is interesting to note that the As 3*d* core-level BE of the reacted component changes by only 0.3 eV to higher values in the investigated coverage range, while the Ga 3*d* PE line of reacted Ga shifts by 0.7 eV to lower BE's. A detailed discussion of these BE variations in connection with current models for the chemical structure of the interface will be given in Sec. V.

The respective Tm 4*f* shallow core-level and valence-band PE spectra are presented in Fig. 2. The as-cleaved semiconductor surface displays the typical triple-peaked structure of the GaAs density of states.[23] After a Tm deposition of 0.2 Å, band bending induces a BE change, which is also clearly observed in the valence-band spectrum. In addition, a strong 4*f* emission from trivalent Tm becomes visible at BE's between 5 and 13 eV. With increasing Tm coverage, this Tm $4f^{11}$ final-state multiplet increases in intensity relative to the GaAs valence band and gradually shifts to lower BE's. Again, an abrupt shift to lower BE's by $\simeq 0.33$ eV occurs at Tm coverages between 2 and 2.8 Å, in accordance with the behavior of the As 3*d* and Ga 3*d* core levels. In the same coverage range, a finite density of states appears at the Fermi level, signaling metallization of the overlayer due to an increasing overlap of the valence-electron orbitals. At still higher Tm coverages, a second Tm $4f^{11}$ multiplet grows at $\simeq 0.6$-eV lower BE, which is assigned to emission from bulk Tm atoms. In addition, we observe that the valence band adopts more and more the typical triangular shape of a 5*d*-derived band, and the BE's of the Tm $4f^{11}$ multiplets approach values typical for elemental

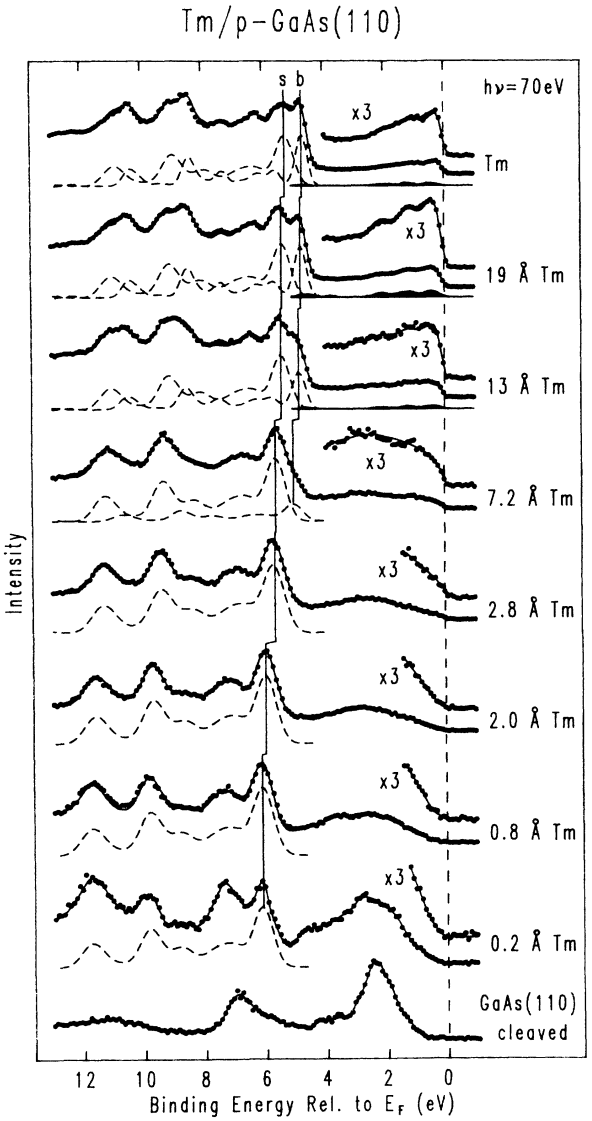

FIG. 2. Photoemission spectra of the Tm/*p*-type-GaAs(110) interface as a function of Tm coverage in the region of the shallow Tm 4*f* core level and the valence band. The notation corresponds to that of Fig. 1. Emission from divalent Tm atoms, as observed at higher coverages (e.g., 19 Å Tm), is given by the weak filled subspectra close to E_F. All spectra are normalized to equal height.

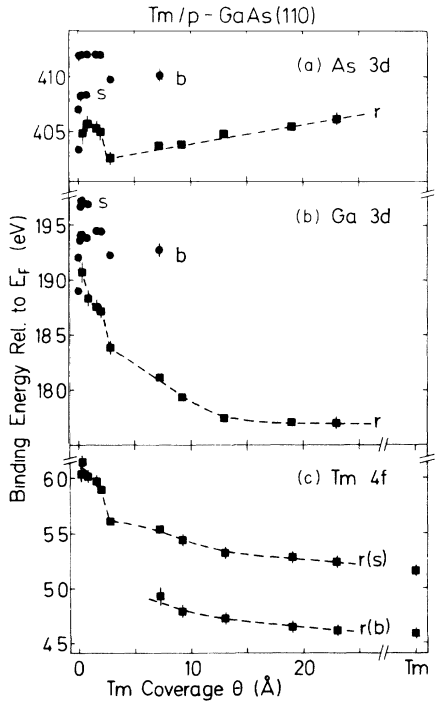

FIG. 3. Binding energies of (a) As 3*d*, (b) Ga 3*d*, and (c) Tm 4*f* PE lines as a function of Tm coverage derived from the spectra in Figs. 1 and 2. The estimated error bars are given in those cases, where they exceed the dimensions of the symbols.

Tm metal. At Tm coverages exceeding $\simeq$13 Å, weak additional spectral features appear in the BE range between 0 and 4 eV, which show the typical triple-peaked structure of the $4f^{12}$ multiplet of divalent Tm.[20] This Tm^{2+} emission exhibits a maximum in relative intensity at Tm coverages of $\simeq$20 Å, with a BE of 0.5 eV for the weakest-bound multiplet component.

The BE's of the As 3*d*, Ga 3*d*, and Tm 4*f* core levels, resulting from a detailed least-squares-fit analysis, are plotted in Fig. 3 as a function of Tm coverage. An inspection of these data clearly shows that the BE shifts of substrate core levels due to defect-induced band bending are completed even at the lowest Tm coverage studied here (0.1 Å). At higher coverages, the substrate BE's remain constant, with the exception of the metallization-induced shift occurring between 2 and 2.8 Å. For the reacted components, all three core levels studied exhibit continuous, smooth BE changes, which are only interrupted by discontinuities due to the metallization-induced shifts.

In Table I, the Gaussian linewidths W, as obtained from the fit analysis, are given for the substrate (W^s) and reacted-layer (W^r) components of both As 3*d* and Ga 3*d* spectra. In general, PE lines from the reacted components are found to be broader than those from substrate atoms, which is interpreted as a consequence of inhomogeneities in chemical composition or coordination in the reacted layer. In addition, a broadening of all PE lines is observed in the Tm-coverage range between 0 and 0.8 Å; this may be a combined effect of lateral inhomogeneities in band bending across the GaAs(110) surface and the known variation in band bending within the PE sampling depth (see Sec. IV). Almost no changes in linewidths, however, are observed in the Tm-coverage range from 2.0 to 2.8 Å, when the metallization of the interface takes place; this applies particularly to the PE lines from substrate atoms. In addition, no evidence for asymmetric line shapes characteristic for electron-hole pair creation in the PE process (Doniach-Šunjić line shape),[24] is found in the spectra for 2.8 Å of Tm, which suggests the presence of only weak metallic character. This finding agrees with the relatively weak emission ob-

TABLE I. Gaussian linewidths W^s and W^r, resulting from the least-squares-fit analysis for the PE lines from substrate atoms (bulk and surface) and atoms in the reacted layer, respectively, of the Tm/*p*-type-GaAs(110) interface; the subscript indices refer to As 3*d* and Ga 3*d* PE lines. The Lorentzian lines used in the convolution were kept at a constant linewidth of 0.2 eV (FWHM), as resulting from the PE spectra of uncovered GaAs(110).

Θ (Å)	W^s_{As} (eV)	W^r_{As} (eV)	W^s_{Ga} (eV)	W^r_{Ga} (eV)
0	0.37		0.30	
0.2	0.41	0.67	0.33	0.56
0.8	0.47	0.75	0.36	0.68
1.6	0.47	0.75	0.35	0.75
2.0	0.47	0.71	0.35	0.75
2.8	0.47	0.66	0.36	0.77
7.2	0.47	0.54	0.39	0.66
9.2		0.54		0.68
13		0.66		0.44
19		0.64		0.41
23		0.71		0.39

served at E_F for $\Theta = 2.8$ Å (see Fig. 2). On the other hand, the Ga 3*d* line shapes of the 13- and 19-Å spectra [see Fig. 1(b)] exhibit tails to higher BE typical for Doniach-Šunjić line shapes. No detailed fit analysis of the line shapes of the reacted-component PE lines at these high coverages, however, was performed, since also strong inhomogeneities in chemical composition and coordination number are expected to contribute.

B. Yb/GaAs(110) interface

In Fig. 4, the As 3*d* and Ga 3*d* core-level PE spectra of the Yb/GaAs(110) interface are shown for different Yb coverages. The overall behavior is very similar to the one observed for the Tm/GaAs(110) interface. With increasing Yb coverage, a growth in the PE signals from reacted components is observed in the spectra. Also, line shifts due to initial band bending are seen for low Yb coverages. In the coverage range between 2.5 and 5.6 Å, additional shifts by $\simeq 0.2$ eV to lower BE are observed for both the Ga 3*d* and As 3*d* PE lines of the reacted component. For the present interface, these shifts could only be monitored in the PE signals of the reacted overlayer, since PE from substrate atoms could not be followed to high enough Yb coverages. The reason for this difference lies in a higher surface sensitivity in the Yb/GaAs(110) PE measurements as compared to those on the Tm/GaAs(110) interface, caused solely by different experimental geometries: The Tm/GaAs(110) spectra were taken in normal-emission geometry, i.e., the effective electron escape depth was equal to the electron mean-free path. On the other hand, the Yb/GaAs(110) data were taken in non-normal geometry with a cylindrical mirror analyzer (CMA), causing a reduction of the effective electron escape depth by a factor of $\simeq 2$.

The corresponding Yb 4*f* PE spectra are presented in Fig. 5. They are dominated by intense $4f^{13}$ final-state doublets from divalent Yb. No intensity is observed in the higher BE range of these spectra (not shown here), where emission from trivalent Yb $4f^{12}$ multiplets would be located. We may therefore state that the trivalent Yb content, if any, is below 3%. In the as-cleaved GaAs(110) spectrum, only weak emission from the valence band of GaAs is observed; upon Yb evaporation, this spectral region is completely dominated by the strong Yb $4f^{13}$ emission, even for the lowest Yb coverages studied. For Yb coverages up to 2.5 Å, the spectra can be well described by a single broad doublet. Between 2.5 and 5.6 Å of Yb, these PE lines shift by $\simeq 0.3$ eV to lower BE, in close analogy to the behavior of the As 3*d* and Ga 3*d* core-level PE lines. The spectra measured for Yb coverages of 5.6 Å and above can no longer be described by a single 4*f* doublet. At a coverage of $\simeq 17$ Å (and beyond), the 4*f* spectrum clearly consists of two doublets that originate from bulk and surface Yb atoms in the reacted layer. The assignment of the respective subspectra in Fig. 5 will be explained in more detail in Sec. V. We note here that the BE of the Yb 4*f* signal increases gradually with increasing metal coverage approaching the values known for elemental Yb metal.

The variation of core-level BE's for Yb coverages in the range from 2.5 and 5.6 Å is similar to the one observed for the Tm/GaAs(110) interface for Tm coverages between 2 and 2.8 Å. Even though a metallization of the Yb/GaAs(110) interface cannot be monitored directly in the valence-band PE spectra of Fig. 5, it is assumed here that the observed additional BE shifts are also caused by a second band bending upon metallization of the interface. The difficulty in monitoring a finite density of states at E_F in the Yb/GaAs(110) interface is mainly related to the high Yb 4*f* density of states close to E_F, as well as to the fact that the conduction electrons of divalent Yb metal are *sp*-like, giving rise to a relatively low PE cross section at the high photon energies employed.

In Fig. 6, the BE variations of the As 3*d*, Ga 3*d*, and Yb 4*f* core levels are shown as a function of Yb coverage, both for substrate atoms and reacted components. The general behavior of the As 3*d* and Ga 3*d* core levels is similar to the one found for the Tm/GaAs(110) interface (see Fig. 3); however, there are also some noticeable differences. (i) The BE shift induced by the second band bending can be followed only for the reacted component;

as explained in more detail above, this is due to the relatively high surface sensitivity of the Yb/GaAs(110) experiments. (ii) The BE behavior of the Yb $4f$ PE signal was found to be different from that of the Tm $4f$ lines: chemical reaction in the interfacial region shifts the Tm $4f$ PE lines from their elemental positions to higher BE's, while the Yb $4f$ signal is displaced to lower BE. This opposite behavior will be explained in Sec. V on the basis of thermochemical arguments. (iii) The observed As $3d$ and Ga $3d$ BE shifts of substrate atoms for low Yb coverages ($1 \leq \Theta \leq 2$ Å) amount to only $\simeq 0.4$ eV as compared to $\simeq 0.5$ eV in case of the Tm/p-type-GaAs(110) interface. This is a consequence of a small initial band bending of the cleaved p-GaAs(110) surface used to prepare the interface with Yb, as revealed by the absolute values of Ga $3d$ and As $3d$ BE's for the uncovered substrate. A correction of the above BE shift ($\simeq 0.4$ eV) for this initial band bending ($\simeq 0.15$ eV) leads then to a band-bending

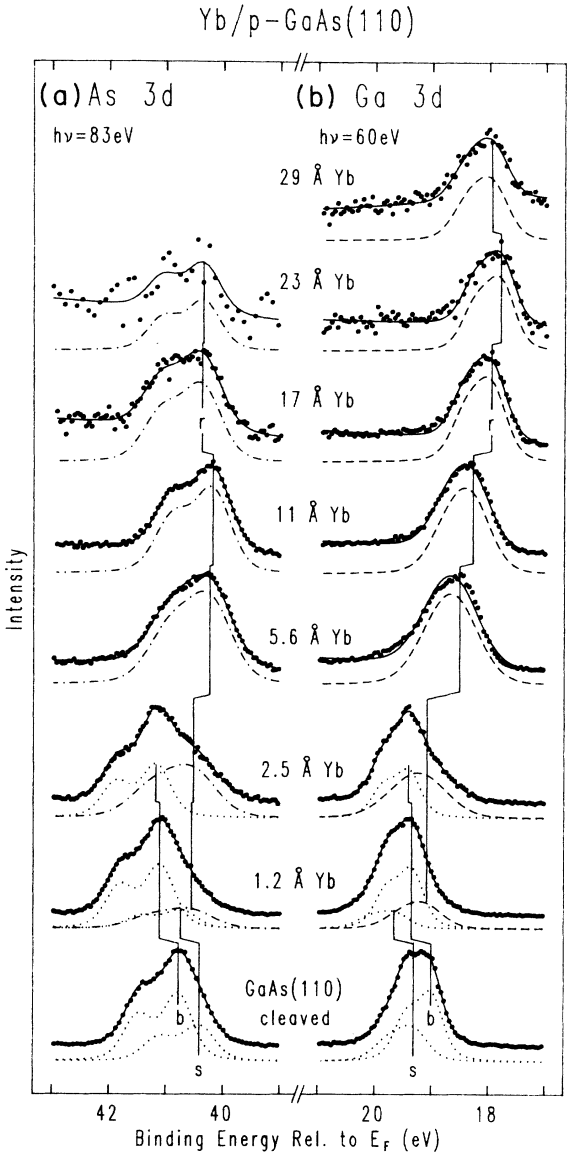

FIG. 4. Photoemission spectra of the Yb/p-type-GaAs(110) interface as a function of Yb coverage, with the signals from (a) As $3d$ and (b) Ga $3d$ core levels plotted separately. The solid lines through the data points represent the results of least-squares fits. The dotted subspectra originate from unreacted GaAs, while the dashed-dotted components stem from interfacial $YbAs_x$, and the dashed signal from $YbGa_x$. All spectra are normalized to equal height.

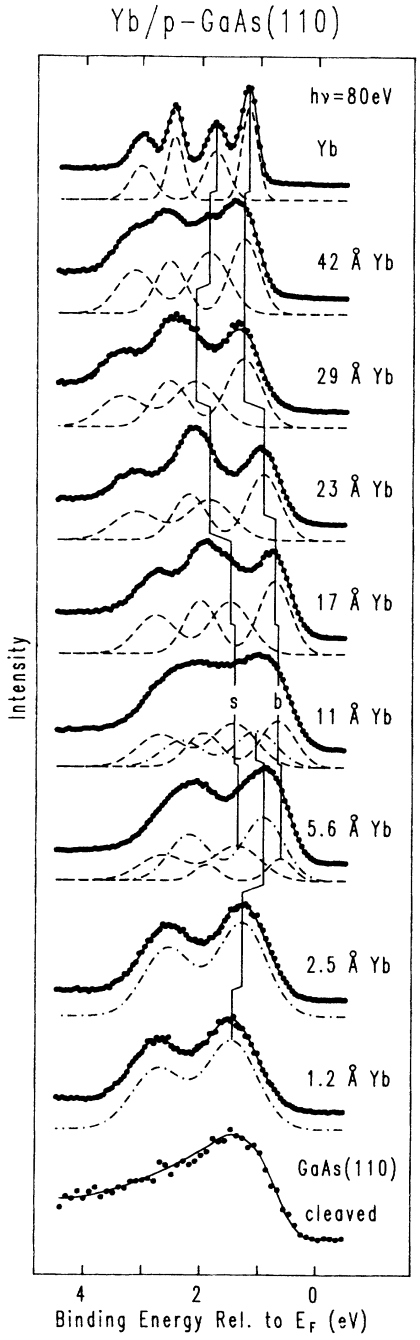

FIG. 5. Photoemission spectra of the Yb/p-type-GaAs(110) interface as a function of Yb coverage in the region of the $4f^{13}$ final-state multiplet from divalent Yb. The notation is the same as in Fig. 4. All spectra are normalized to equal height.

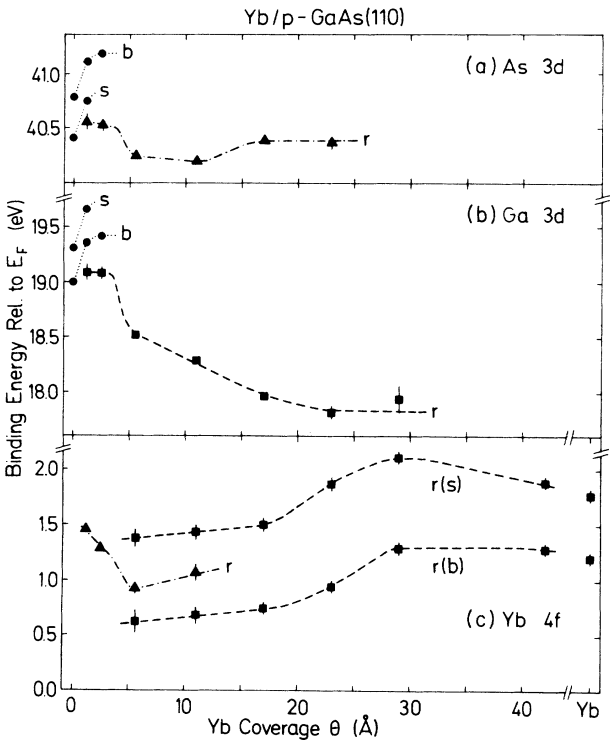

FIG. 6. Binding energies of (a) As 3*d*, (b) Ga 3*d*, and (c) Yb 4*f* PE lines for the different subspectra in Figs. 4 and 5, plotted as a function of Tm coverage. The same notation of the line symbols as in Figs. 4 and 5 is used in order to distinguish the different chemical phases in the interfacial region. Error bars are given where they exceed the dimensions of the symbols.

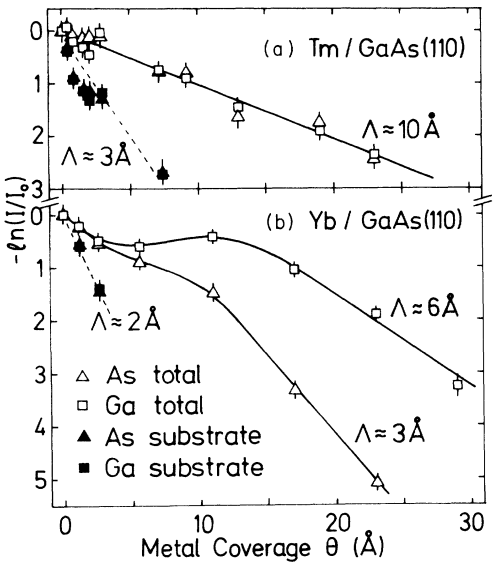

FIG. 7. Semi-logarithmic plot of intensities of the As 3*d* and Ga 3*d* total spectra (solid lines) and of the subspectra from the unreacted GaAs substrate (dashed lines), as a function of metal coverage. The intensities are normalized relative to uncovered GaAs. Attenuation lengths Λ, corresponding to approximately linear parts of the curves, are also given. Note that the effective electron escape depth is $\lambda \simeq 6$ Å for Tm/GaAs(110) and $\lambda \simeq 3$ Å for Yb/GaAs(110); this is mainly due to the different geometries employed in the present PE experiments on these two interfaces.

value for the Yb/*p*-type-GaAs(110) interface at low coverage ($1 \leq \Theta \leq 2$ Å) in close agreement with the one observed for Tm/*p*-type-GaAs(110).

A further noteworthy difference between the two interfaces is contained in the observation that for Yb/GaAs(110), Ga 3*d* emission is still visible at such high metal coverages, where As 3*d* emission has already become undetectable. This is readily seen by inspection of Fig. 7, where the intensities of the As 3*d* and Ga 3*d* PE signals are plotted in a semilogarithmic way versus metal coverage for both interfaces. While in case of the Tm/GaAs(110) interface, the As 3*d* and Ga 3*d* intensities are almost equal, they behave in rather different way as a function of metal coverage for the Yb/GaAs(110) interface: At coverages exceeding 3 Å, the Ga 3*d* intensity is substantially higher than the As 3*d* intensity. This behavior must be due to a different diffusive behavior of As and Ga atoms at the two interfaces: For the Yb/GaAs(110) interface, the As atoms seem to stay close to the interface, while the Ga atoms tend to diffuse to the surface. This leads to the observed difference in As 3*d* and Ga 3*d* PE intensities as a function of coverage for the reacted layer. We interpret this observation by postulating the existence of two different compounds: A $YbAs_x$ compound near the interface and a $YbGa_x$ alloy piled up close to the surface. This is definitely an oversimplified model, since—in reality—atomic diffusion will be incomplete and therefore also ternary compounds should be formed. Nevertheless, there will be a certain preference in forming spatially separated binary compounds. We have therefore assigned the reacted As 3*d* emission to $YbAs_x$, and the reacted Ga 3*d* emission to $YbGa_x$. The coverage dependences of these intensities, as well as the closely related behavior of the core-level BE's for other RE/GaAs(110) interfaces studies so far, enable us to propose a model for the structure of RE/GaAs(110) interfaces, which will be presented in more detail in Sec. V.

IV. BAND-BENDING BEHAVIOR AND MODELS FOR SCHOTTKY-BARRIER FORMATION

In this section we shall concentrate on the shifts in core-level BE's as a function of metal coverage both for substrate atoms and atoms in the chemically reacted products. For the Tm/GaAs(110) interface, these shifts and their implications for models on Schottky-barrier formation have already been described in a recent letter.[17] Even though our most complete data set is available for the Tm/GaAs(110) interface, we present this subject of considerable interest here in more detail and also compare with the less complete data for the Yb/GaAs(110) interface. Also, additional resonance-lamp spectra for the Ga 3*d* core levels and the valence-band region of interfaces of Tm with *n*- and *p*-type GaAs(110) are presented. These data were taken (i) to

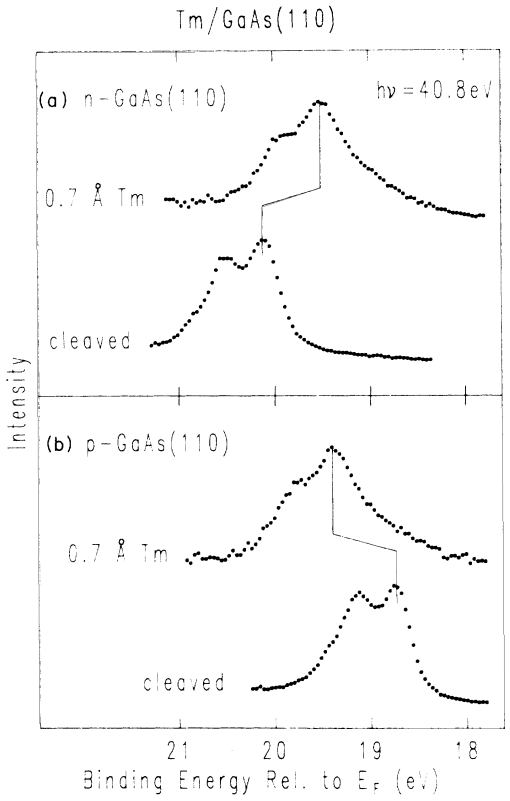

FIG. 8. Ga 3*d* PE spectra taken with He II radiation from cleaved *n*- and *p*-type GaAs and interfaces formed by deposition of 0.7 Å at room temperature. The solid vertical bars represent the positions of the $3d_{5/2}$ core-level PE lines. Note the BE changes in opposite direction for *n*- and *p*-type substrates upon deposition of Tm. The spectra shown were corrected for background from He I light; they are normalized to equal height.

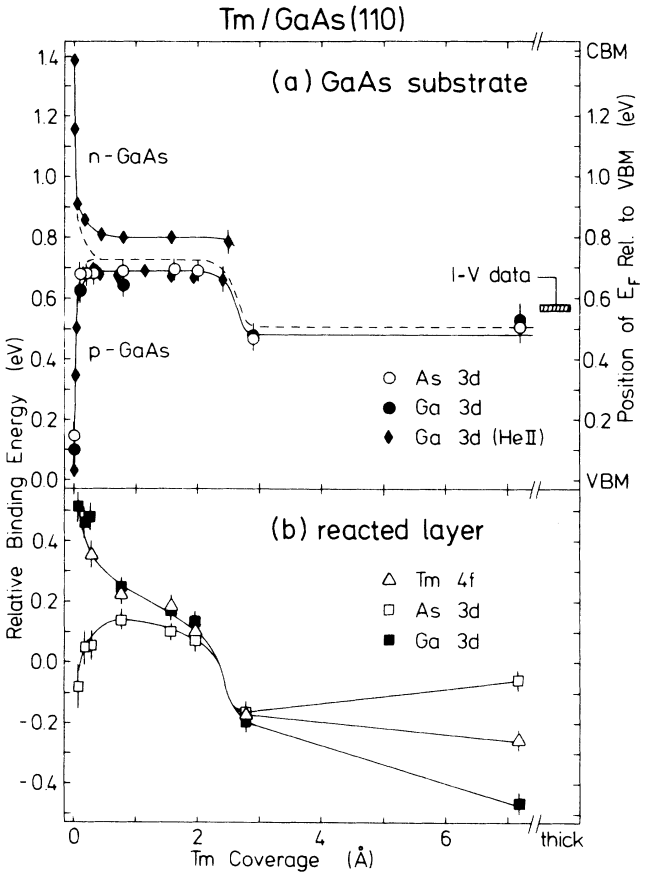

FIG. 9. Core-level BE shifts of the Tm/GaAs(110) interface as a function of Tm coverage for both *n*- and *p*-type substrates: (a) As 3*d* and Ga 3*d* from atoms in the GaAs substrate; (b) Tm 4*f*, As 3*d*,and Ga 3*d* core levels from atoms in the reacted interfacial region. Note the parallel shifts of all core levels to lower BE's at a Tm coverage of $\simeq 2.6$ Å. The dashed line represents the common Fermi-level position for *n*- and *p*-type GaAs obtained from the PE data after correction for finite sampling depths (right-hand scale). The Fermi-level position derived from *I-V* measurements on thick diodes is indicated by the hatched horizontal bar.

complement the synchrotron-radiation data for *p*-type GaAs(110) with corresponding results for *n*-type GaAs(110) and (ii) to further support the metallization of the interface in the range from 2 to 2.8 Å.

A selection of Ga 3*d* PE spectra ($h\nu = 40.8$ eV), which were taken in order to precisely locate the Fermi-level pinning position in the semiconductor band gap for both *n*- and *p*-type GaAs(110), is given in Fig. 8. Note the shifts of the Ga 3*d* PE lines in opposite directions for *n*- and *p*-type substrates due to band bending, which is caused by pinning of the Fermi level to positions close to the center of the semiconductor band gap. The core-level BE's of the three elements studied are presented in Fig. 9 for the Tm/GaAs(110) interface in the coverage range up to $\simeq 7.2$ Å Tm, where PE signals from substrate-atom core levels could still be identified. The data for substrate core levels [Fig. 9(a)] include both the results of the synchrotron-radiation studies of Tm/*p*-type-GaAs(110) (see Figs. 1 and 3) and those of the He II studies for *n*- and *p*-type GaAs(110) substrates. The core-level binding energies of all those atoms in the chemically reacted products are also presented in Fig. 9(b). These data were derived from the synchrotron-radiation studies with *p*-type GaAs(110) substrates (Figs. 1 and 2) and are already included in the plots of Fig. 3 covering a much larger range of Tm exposures. The most striking information contained in Fig. 9 concerns the initial band-bending–induced shifts of substrate core levels for $\Theta < 0.5$ Å, and an additional parallel shift of all core levels to lower BE's at $\Theta \simeq 2.6$ Å occurring in a narrow coverage range.[17] These additional shifts could only be studied with synchrotron radiation, since the higher surface sensitivity of the He II PE measurements does not allow a deep enough sampling of the interface for the required high Tm coverages.

We first address the compatibility of the Fermi-level pinning positions derived for *n*- and *p*-type GaAs(110) substrates from PE experiments. It is striking that band bending stays constant in the initial pinning range of Tm

coverages from $\simeq 0.5$ to $\simeq 2.0$ Å. The Ga $3d$ substrate core-level BE's determined by PE differ for n- and p-type substrates by 0.12 eV [see Fig. 9(a)]. This does not mean that two different Fermi-level positions exist for n- and p-type substrates, but it is rather a consequence of band bending and the finite PE sampling depth.[17,25] This difference may be quantitatively accounted for if the relatively long-range variation of band bending with distance from the interface, extending to typically hundreds of angstroms,[26] and the effective electron escape depth λ of photoelectrons in GaAs ($\lambda \simeq 10$ Å at a kinetic energy of $\simeq 20$ eV)[19] are considered. The observed BE's in the PE spectra are then weighted mean values over the PE sampling depth. In order to obtain a value for the band bending directly at the interface Φ_B, a correction $\Delta\Phi_B$ has to be applied to the PE results. Assuming a linear variation of band bending with distance from the interface, we obtain: $\Delta\Phi_B = \lambda\ (2ne\Phi_B/\epsilon\epsilon_0)^{1/2}$ (see Ref. 26). This means that the PE BE deviates by $+0.08$ eV for n-type GaAs and -0.05 eV for p-type GaAs from the correct BE at the interface (defining the band bending at the interface). In the expression for $\Delta\Phi_B$, ϵ is the dielectric constant of GaAs ($\epsilon = 10.4$) (Ref. 26) and n stands for the concentration of doping atoms. The two sets of data for n- and p-type GaAs substrates then define a single Fermi-level position [dashed line in Fig. 9(a)] at 0.72 ± 0.03 eV above the valence-band maximum for the initial pinning range of Tm coverages from 0.5 to $\simeq 2.0$ Å.

The final Fermi-level position reached after the second band bending at a Tm coverage of $\simeq 2.6$ Å is compared in Fig. 9(a) with the result derived from current-voltage (I-V) measurements on Schottky diodes of the trivalent RE metals Tb, Dy, and Er with n-type GaAs(001): $\Phi_B = 0.85 \pm 0.01$ eV.[27] We may adopt this Fermi-level position for the present Tm/GaAs(110) interface, since all trivalent rare-earth metals are chemically very similar and the Schottky-barrier height is known to be rather independent of the crystallographic orientation of the substrate surface.[8] The Fermi-level position obtained from I-V measurements, given by the hatched horizontal bar in Fig. 9(a), agrees within our experimental accuracy of $\simeq 0.05$ eV with the final Fermi-level position derived from PE spectra of thick metallic Tm overlayers on GaAs(110), but not with the initial position reached at low coverages below $\simeq 2.6$ Å.

The main point of this section concerns the additional parallel shifts of all core levels to lower BE's at $\Theta \simeq 2.6$ Å, when the overlayer metallizes (see Fig. 9). Similar shifts were previously observed for interfaces of other RE metals (Ce, Sm, and Yb) with n-type GaAs(110), but only for core-level PE lines from reacted phases, since substrate core levels were not monitored at relevant coverages.[14–16] These shifts, however, were previously interpreted in terms of chemical effects, which can be excluded in the present case of Tm/GaAs(110) due to the observed parallel shifts in all core levels including those of substrate atoms. We also exclude charging of the whole sample as well as shifts due to possible cluster formation as origins of these additional shifts: Charging effects would depend on photon flux, which was tested and not observed. The reported self-energy effects of metallic clusters on top of an insulating substrate,[28] which get positively charged by PE, would influence core levels of cluster atoms and the position of the Fermi level in a similar way, but with smoothly decreasing shifts to lower BE with increasing cluster diameter (exposure). This is clearly not seen in the present interface.

Before further discussing the parallel shifts of core-level BE's at Tm coverages of $\simeq 2.6$ Å, one has to realize that these shifts occur when the interface assumes metallic character. This has already been pointed out in Sec. III A on the basis of the valence-band PE data taken at $h\nu = 70$ eV (see Fig. 2). We have further studied this correlation by He I PE measurements, where the higher PE cross sections of valence-band states as well as a higher resolution ($\simeq 40$ meV) result in an increased sensitivity. The results are summarized in Fig. 10 and confirm the metallization of the interface at Tm coverages when the abrupt parallel shifts of all core-level BE's are observed.

We therefore identify these shifts as metallization induced, and end up with two further possible origins: (1) A change in band bending due to the metallization of the interface, or (2) metallic screening of core holes in the PE process that would also lead to shifts to lower BE.[29,30] The second mechanism is unlikely to cause the main effect, since both substrate-atom and overlayer-atom core level BE's are affected in almost the same way, which is typical for changes in band bending.[22] The strongest

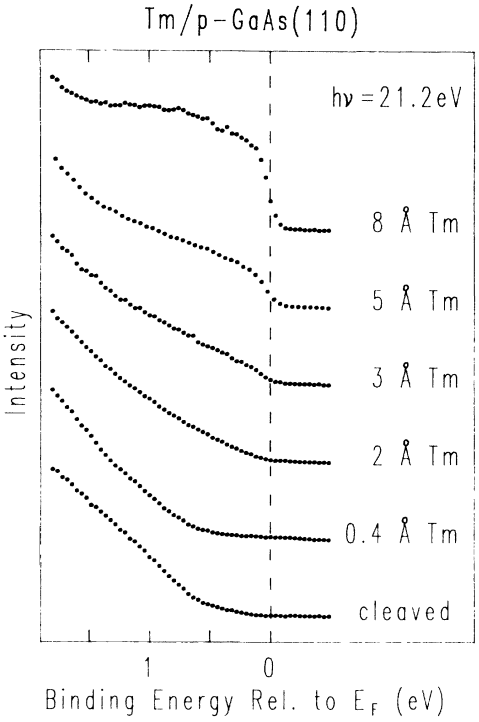

FIG. 10. Valence-band PE spectra of the Tm/p-type GaAs(110) interface for various Tm coverages, taken with He I radiation. Metallization of the interface is reflected in the finite density of states at E_F observed for Tm coverages $\Theta > 2$ Å. All spectra are normalized to equal height.

support of mechanism (1) is provided by the agreement of the Fermi-level position from *I-V* measurements with the final PE BE's of the present experiments for thick metallic Tm overlayers, as discussed above [see also Fig. 9(a)]. Metallic-screening effects would cause systematic deviations to lower BE's, which cannot be larger than the present experimental accuracy of $\simeq 0.05$ eV. The dominant mechanism is therefore identified as a second band bending occurring when the interface metallizes.

A second metallization-induced change in band bending (Fermi-level position) is also clearly visible for the Yb/GaAs(110) interface on the basis of the variations of core-level BE's as a function of Yb coverage plotted in Fig. 6. As discussed above, this data set is less complete than the one for the Tm/GaAs(110) interface, since the substrate-atom core levels could not be followed to high enough Yb coverages in these early investigations mainly for experimental reasons. Nevertheless, a parallel shift of the As 3*d*, Ga 3*d*, and Yb 4*f* core-level BE's to lower values by $\simeq 0.3$ eV is clearly observed for Yb coverages in the range $2.5 < \Theta < 5.6$ Å (see Fig. 6).

The present results for the variation of band bending with metal coverage, in particular the observation of a second band bending upon metallization of the interface, which defines a Fermi-level position in agreement with the results of *I-V* measurements on thick Schottky diodes, has considerable impact on the theoretical models proposed for the formation of Schottky barriers.[2–8] The experimental results on the variation of the Fermi-level position in the Tm/GaAs(110) interface as a function of Tm coverage (Fig. 9) clearly show the existence of two pinning positions. The initial Fermi level for $0.5 < \Theta < 2$ Å lies 0.72 ± 0.03 eV above the valence-band maximum, while the final position after interface metallization for $\Theta > 2.6$ Å is situated $\simeq 0.22$ eV lower, in good agreement with the results of *I-V* measurements. Defect-level pinning[8] may well be responsible for the initial band bending and the Fermi-level position in the low-coverage range up to $\simeq 2.0$ Å Tm, but is very unlikely capable of accounting for the abrupt change in band bending at $\Theta \simeq 2.6$ Å. Even though a switching between different defect levels has been discussed for interfaces formed on InP,[31] such a mechanism is both unexpected for GaAs and would require much stronger chemical changes than reflected in the present PE spectra. It seems therefore obvious to conclude that the abrupt shifts at $\Theta \simeq 2.6$ Å are caused by metallization of the interface leading to an overcompensation of defect pinning states. One such mechanism, proposed by Heine, Tersoff, and Flores,[5–7] is based on metal-induced gap states (MIGS) in the band gap of the semiconductor close to the interface. This MIGS model of Schottky-barrier formation is consistent with the present results.

In the following, the presently available results on the behavior of band bending as a function of metal coverage are briefly discussed in a comparative way for the RE/GaAs(110) interfaces. We first note that the magnitude of the defect-level induced band bending at low metal coverages observed in the present work for Tm/*n*-type-GaAs(110) ($\Phi_B = 0.68 \pm 0.03$ eV) agrees within ± 0.07 eV with the results reported for other RE/*n*-type-GaAs(110) interfaces: 0.73 eV for Ce,[14] 0.63 eV for Sm,[15] and 0.61 eV for Yb.[16] This close agreement suggests the creation of similar defect states when the various RE metals react chemically with GaAs(110). Such a behavior is actually expected from the chemical similarity of the RE elements.

In previous studies of interfaces between Ce, Sm, and Yb with *n*-type GaAs(110), PE signals from substrate-atom core levels were not monitored for sufficiently high RE coverages in order to allow the observation of metallization-induced BE shifts.[14–16] This was presumably due to the surface-sensitive experimental geometries employed in these former studies. On the other hand, for atoms in the reacted interfacial layers, shifts of the PE signals by $\simeq 0.2$ eV to lower BE's were also observed for all RE/GaAs(110) interfaces at RE coverages between 2 and 7 Å. These shifts closely resemble the metallization-related band-bending shifts described in the present paper; they were interpreted, however, in terms of a transition from a weakly reacted to a fully reacted phase.[14–16] In view of the present results, such an interpretation in terms of a chemical change has become questionable. The present interpretation suggests then a more gradual change in interfacial chemistry with increasing RE coverage for all RE/GaAs(110) interfaces studied so far.

It should also be noted that the *initial* Fermi-level position as determined by defect states is approximately the same for all reactive interfaces with GaAs(110) investigated up to now,[8] not just for those with RE metals. This is actually suggested by the similar character of defect states created by various metals on GaAs(110).[8] On the other hand, the *final* Fermi-level position, which is determined by MIGS, should depend on the particular metal deposited due to the following reasons. (i) The charge-neutrality level of the MIGS (Refs. 6 and 7) depends on the valence-band structure of the metal in contact with the semiconductor; particularly transition metals exhibit large variations in band structure as a consequence of the different *d*-electron contributions. (ii) Different work functions of the metals will lead to a variation in the separation between the Fermi level and the charge-neutrality level of the MIGS.[6,7] (iii) In the reactive case, compounds or alloys are formed at the interface allowing therefore a further variation in Fermi-level position.

Thus, a relatively abrupt transition of the Fermi level from defect-level pinning to MIGS pinning upon interfacial metallization, as observed here, cannot be expected generally for interfaces of metals with GaAs(110). In fact, related shifts at similar metal coverages have only been observed for reactive interfaces with Au, Ti, Y, and Na.[32–35] It is beyond the scope of the present paper to judge the various reasons, which could be responsible for not observing additional MIGS-induced shifts in some of the other studied reactive metal-GaAs(110) interfaces. They include both less bulk sensitivity of the PE measurements and a possible accidental coincidence of defect-induced and MIGS-induced Fermi-level positions. In addition, some of the previous studies may lack the required accuracy in data acquisition or analysis. With the results presented in this work, however, a dominance of MIGS

pinning has to be assumed for relatively high metal coverages, and therefore also for realistic Schottky contacts.

V. STRUCTURE OF RARE-EARTH/GaAs(110) INTERFACES

A comparison of the coverage dependences of the As 3*d* and Ga 3*d* core-level BE's presented in Figs. 3 and 6 for the Tm/GaAs(110) and Yb/GaAs(110) interfaces, and also for the Ce/GaAs(110) (Ref. 14) and Sm/GaAs(110) (Ref. 15) interfaces studied previously, shows that similar chemical structures characterize the growth of these interfaces. This is a consequence of the closely related chemical properties of the RE elements, with their localized 4*f* electrons that usually do not participate in chemical bonding. In the Yb/GaAs(110) interface, a spatial separation of As and Ga atoms takes place in the reacted layer, as can be inferred from the intensity-versus-coverage behavior [Fig. 7(b)]. The corresponding data for the Tm/GaAs(110) interface [Fig. 7(a)] are not revealing such a separation. Nevertheless, the coverage dependences of the core-level BE's follow similar trends in both interfaces (Figs. 3 and 6), an observation that suggests also the formation of separate $TmAs_x$ and $TmGa_x$ compounds in the Tm/GaAs(110) interface. In the Tm case, however, the reaction products appear not to be spatially separated in the direction normal to the interface. This view is supported by the intensity-versus-coverage dependences observed for the Ce/GaAs(110) (Ref. 14) and Sm/GaAs(110) (Ref. 15) interfaces, where only minor differences were found for the coverage dependences of the As 3*d* and Ga 3*d* PE intensities. If we exclude Ce in the series of investigated RE/GaAs(110) interfaces, because of its different 4*f*-related chemical behavior, there is a clear trend in this series. The spatial separation of As and Ga normal to the surface increases from trivalent Tm via less stable trivalent Sm (where the surface is divalent) to divalent Yb. On the other hand, it is presently difficult to give a theoretical explanation for this behavior, since data on surface energies of the respective compounds as well as diffusion coefficients are not available.

In the following, we will present a model for the chemical structure of RE/GaAs(110) interfaces: In all cases, the reacted components with As exhibit only weak variations of BE with metal coverage, suggesting relatively constant stoichiometries of the RAs_x compounds. The existence of elemental As may be excluded on the basis of the observed PE spectra, since the BE of elemental As (41.7 eV) (Ref. 36) is more than 1-eV higher than those observed for the various RAs_x phases. On the other hand, the relatively strong variations in BE observed for the PE lines from Ga-containing reacted phases hint to much stronger changes in stoichiometry: Since the BE of elemental Ga (18.7 eV) (Ref. 36) agrees quite well with those observed for the Ga phases in the RE/GaAs(110) interfaces at low metal coverages, we assign the reacted Ga 3*d* PE line at low metal coverages to segregated elemental Ga. With increasing metal coverage, the RE content increases in the RGa_x alloy phases, causing the relatively large BE shifts observed. This view is further supported by the RE-Ga phase diagrams, which contain a variety of compounds with different stoichiometries,[37] whereas the RE-As phase diagrams are characterized by much fewer compounds.[38] Due to inhomogeneities in chemical composition, the Ga 3*d* lines are broadened with respect to the substrate lines in the range of large BE changes, and at higher coverages, the line shape of a single doublet is not sufficient to fit the data well (see Figs. 1 and 4 and discussion in Sec. III A). The As 3*d* lines are narrower due to the smaller BE shifts, but they are generally broader than the substrate lines (see Table I).

The BE's of the As 3*d* PE lines of the RAs_x compounds exhibit only minor variations to larger values with increasing metal coverage for all investigated RE/GaAs(110) interfaces (see Figs. 3 and 6 and Refs. 14 and 15). This behavior could originate from several mechanisms. In case of the Ce/GaAs(110) (Ref. 14) and Sm/GaAs(110) (Ref. 15) interfaces, it was proposed that a fully reacted As component with a low As 3*d* BE is trapped at the interface, and a surface segregation of an As species with $\simeq 0.3$ eV higher BE takes place. The latter species dominates at higher coverages, leading to the observed shifts. On the other hand, minor variations in stoichiometry as well as changes in coordination number may lead to the observed shifts. From the present results, it does not seem possible to decide between these various possibilities.

As can be seen in Fig. 2, a separation into two different Tm compounds cannot be inferred from the Tm 4*f* PE spectra alone. This is essentially a consequence of limited resolution, since chemically-induced BE shifts in this case are not exceeding $\simeq 0.4$ eV. Possible BE differences between $TmAs_x$ and $TmGa_x$ phases are therefore too small to allow a separation of the Tm 4*f* PE signals within the experimental resolution.

On the other hand, the Yb 4*f* PE lines experience stronger chemical shifts, and this then allows an identification of separate As and Ga compounds of Yb (see Fig 5). For Yb coverages up to $\simeq 2.5$ Å, the spectra may be described by one broad 4*f* doublet assigned to $YbAs_x$. With increasing Yb coverage, this doublet shifts slightly to lower BE's probably due to an increasing mean coordination of the Yb atoms. For such low coverages, the $YbGa_x$ phase is very rich in Ga, and will therefore contribute only in a negligible way to the Yb 4*f* PE spectrum. At an Yb coverage of $\simeq 5.6$ Å, the Yb 4*f* doublet is found to be shifted to $\simeq 0.3$ eV lower BE, which is assigned to a change in band bending due to metallization of the interface (see Sec. IV). The PE spectrum at 5.6 Å clearly exhibits a shoulder on the high-BE side, which is a fingerprint of the $YbGa_x$ alloy phase visible only for such relatively large Yb coverages. Since this phase is located predominantly in the region close to the surface, the Yb 4*f* spectra at still higher Yb coverages are increasingly dominated by emission from $YbGa_x$; both a surface component and a growing bulk component may be distinguished. It should be noted here that especially the Yb 4*f* spectrum observed for an Yb coverage of $\simeq 11$ Å cannot be fitted with less than three 4*f* doublets: In this

case, $4f$ signals from $YbAs_x$ (which is a bulk feature due to the covering $YbGa_x$ phase) and from the $YbGa_x$ phase, separated into bulk and surface contributions, may be distinguished. At higher coverages, the signal from $YbAs_x$ gets too weak to be followed, in agreement with a decline in the As $3d$ intensity. In addition, the $YbGa_x$ phase becomes increasingly richer in Yb, resulting in a movement of the surface and bulk $4f$ doublets towards the BE's known for elemental Yb metal.[21]

In a previous study of the Yb/GaAs(110) interface,[16] very similar Yb $4f$ spectra were reported, but differently assigned in the intermediate coverage range. It was stated that the Yb $4f$ emission from the $YbAs_x$ phase has a lower BE than the bulk $YbGa_x$ component. The general behavior of our spectra in the coverage range between 5.6 and 17 Å, where no data were presented in Ref. 16, does not support such an interpretation.

We are now in a position to discuss the different BE behaviors observed for the RE $4f$ multiplet spectra. First, we note that despite the similar behavior of the As $3d$ and Ga $3d$ spectra, the $4f$ spectra exhibit different trends with RE exposure for Sm and Tm on one side and Yb on the other side: The interaction with GaAs shifts the $4f$ levels of trivalent Sm and Tm to higher BE with respect to the elemental metals, while the $4f$ doublet of divalent Yb is shifted into the opposite direction to a somewhat higher extent (see also Ref. 15). This seemingly peculiar behavior arises from the different valences of these RE ions, as will be shown in the following on the basis of thermochemical arguments.

The BE of the $4f$ state measured by PE is given by the energy difference between the initial and final states. In the PE process, a $4f$ core electron is ejected, leading to an effective increase of the valence of the final-state ion by one, if complete screening through valence electrons is assumed. For a compound, the valence change yields a difference in the heats of formation, ΔH, of the initial (i) and the final (f) state, and hence a BE shift S of the $4f$ core level with respect to the value of the elemental metal[39]

$$S = E_B^{\text{com}} - E_B^{\text{metal}} = \Delta H(f) - \Delta H(i) + E_{\text{imp}}^{\text{com}} - E_{\text{imp}}^{\text{metal}} \quad . \quad (1)$$

Here E_B^{com} and E_B^{metal} represent the BE of compound and elemental metal, respectively, and E_{imp} denotes the heat of solution of the final-state ion in the matrix of the ground-state ions (impurity term). In case of elemental RE metals, this term amounts to 0.5 eV, independent of valence,[40] and it is expected to be smaller for compounds. Thus, the sign of the BE shifts is given mainly by the sign of the difference of the formation enthalpies ΔH in the initial and final state. This quantity may be calculated using the semiempirical scheme of Miedema:[41] Since formation enthalpies are not available for the RE metals, one usually replaces a divalent RE ion by Ca, a trivalent one by Y, and a tetravalent one by Hf.[39] In this way one obtains positive values of up to 0.5 eV for a trivalent initial state and negative values of up to 0.9 eV for a divalent initial state of a RGa_x or RAs_x compound, with the magnitude of the shift depending on stoichiometry. This result is very similar to the one derived previously for RE dialuminides.[39] In this way—assuming a mutual cancellation of the two impurity terms—shifts to higher BE of up to $+0.5$ eV are expected for trivalent Sm and Tm, while shifts to lower BE of up to -0.9 eV are predicted for divalent Yb. This theoretical range for the BE shift S is in excellent agreement with experimental observations.

The lowest Yb $4f$ BE observed is 0.5 eV and therefore of the order of the impurity term. This means that the trivalent state of Yb is almost reached. In case of the Yb/Si(111) interface, the $4f^{12}$ final-state multiplet, characteristic for trivalent Yb, has been observed in the reported PE spectra, increasing strongly in intensity, upon thermal annealing.[10] On the other hand, for the Yb/Ge(111) (Ref. 13) and Yb/GaAs(110) (Ref. 16) interfaces no trivalent $4f$ emission has been observed with the interfaces formed at room temperature. It should be noted here that the Yb $4f$ BE's calculated with Miedema's scheme are very similar for the binary systems Yb-Si, Yb-Ge, Yb-As, and Yb-Ga. This then suggests that thermal treatment of the interfaces could also lead to valence transitions in the Yb/Ge(111) and Yb/GaAs(110) interfaces. Such experiments have not been performed yet.

In the present study, the surface core-level shift of the Yb $4f$ level in the $YbGa_x$ compound was found to be 0.75 eV at low coverages, which is larger than the known value for elemental Yb metal (0.55 eV).[21] This is caused by the higher cohesive energies of RE compounds with $4f$ BE's lower than that of the elemental metal. Therefore, a decrease of the surface core-level shift is expected for increasing metal coverages. The PE spectra obtained for coverages around 30 Å (see Figs. 5 and 6), however, exhibit particularly high surface core-level shifts up to 0.9 eV, despite the observation that the bulk BE's are close to that of elemental Yb metal. Also, the intensities of the reacted As $3d$ and Ga $3d$ components show that the As and Ga atom concentrations at the surface cannot be higher than 5% at $\Theta \simeq 30$ Å. These observations show that these particularly high surface core-level shifts cannot be explained by chemical differences between bulk and surface atoms, but may instead be ascribed to surface roughening. Similar spectra were also observed for the Yb/Si(111) (Ref. 42) and Yb/Ge(111) (Ref. 13) interfaces at comparable coverage, where the elemental-metal layer starts to grow. At this stage of overlayer growth, no long-range crystal structure is yet established, and the average coordination number of surface atoms of the small crystallites formed should be lower than on a smooth surface. Therefore, the surface core-level shifts are expected to be higher.[21] In the case of Tm/GaAs(110), an enhanced surface roughening leads to a valence transition to the divalent state at the low-coordinated edge and corner sites.[43] This effect is readily visible in Fig. 2 in the $\Theta \simeq 19$ Å spectrum; from the observed intensities it is estimated that $\simeq 10\%$ of the surface Tm atoms are in the divalent state. Because of the occurrence of this valence transition, no enhanced surface core-level shift is observed in the Tm $4f^{11}$ multiplet spectra of trivalent Tm (see Fig. 2).

In contrast to the RE core-level spectra, the reacted components in the Ga $3d$ and As $3d$ spectra are not exhibiting surface core-level shifts. This can be either due to a RE termination of the surfaces, or possible surface components are not resolved from the bulk signals due to the large experimental linewidths as compared to typical As $3d$ and Ga $3d$ surface core-level shifts.[19]

VI. CONCLUSIONS AND OUTLOOK

From the present results, general conclusions on the formation of Schottky barriers as well as on the chemical and structural behavior of RE/GaAs(110) interfaces were drawn. It was shown that the Schottky barrier, as observed in thick Schottky diodes, does not form at interfaces between GaAs and a thin metal overlayer before the interface has metallized. This observation was interpreted in support of the metal-induced gap-states models describing Fermi-level pinning in such metal-semiconductor interfaces. In this respect, the present results are expected to have considerable impact on the subject of metal/semiconductor interfaces.

The second main result of the present work concerns the chemical structure of RE/GaAs(110) interfaces and trends connected with the $4f$ electronic structure (valence) of the RE metals. It was shown that chemical reactions take place even in the submonolayer regime, leading to a spatial separation of As and Ga atoms in the interface. A $R\mathrm{As}_x$ phase with a relatively constant stoichiometry is formed as well as a $R\mathrm{Ga}_x$ alloy with a Re R content that increases with RE coverage. The products of this chemical reaction are found to change in a continuous way as a function of RE coverage. For divalent and trivalent RE metals on GaAs(110), the BE's of the $4f$ multiplets shift in opposite directions away from the values known for the elemental metals, an observation, which is quantitatively explained in the thermochemical scheme of Miedema. Detailed analysis of surface core-level shifts of Yb $4f$ lines as well as the observation of a partial surface valence transition in case of Tm show that the elemental RE metal films, starting to grow for metal coverages of $\Theta > 20$ Å (Tm) and $\Theta > 30$ Å (Yb), are characterized by rough surfaces, which turn smoother at higher coverages.

It is quite clear that the present observation of a metallization-induced change in Fermi-level position in metal/semiconductor interfaces requires further experimental verification, particularly in less reactive interfaces. As mentioned above, similar BE changes had been reported earlier for RE/semiconductor interfaces.[14–16] but were differently interpreted. In the course of the present work, related changes in band bending upon interface metallization were also reported for interfaces between transition metals and GaAs.[44]

ACKNOWLEDGMENTS

The authors thank G. Kalkowski, T. Mandel, and E. Weschke as well as the staff of BESSY/Berlin for assistance during the measurements. This work was supported by the Bundesminister für Forschung und Technologie (Projekt No. 05-313AX-B2/TP3), Bonn, Germany.

[1]L. J. Brillson, Surf. Sci. Rep. **2**, 123 (1982).
[2]W. Mönch, Phys. Rev. Lett. **58**, 1260 (1987).
[3]W. Schottky, Z. Phys. **118**, 539 (1942).
[4]J. L. Freeouf and J. M. Woodall, Appl. Phys. Lett. **39**, 727 (1981).
[5]V. Heine, Phys. Rev. **138**, A1689 (1965).
[6]J. Tersoff, Phys. Rev. Lett. **52**, 465 (1984).
[7]F. Flores and C. Tejedor, J. Phys. C **20**, 145 (1987).
[8]I. Lindau and T. Kendelewicz, CRC Crit. Rev. Solid State Mater. Sci. **13**, 27 (1986).
[9]See, e.g., *Valence Instabilities*, edited by P. Wachter and H. Boppart (North-Holland, Amsterdam, 1982).
[10]G. Rossi, D. Chandesris, P. Roubin, and J. Lecante, Phys. Rev. B **33**, 2926 (1986); G. Rossi, J. Nogami, J. J. Yeh, and I. Lindau, J. Vac. Sci. Technol. B **1**, 530 (1983).
[11]A. Franciosi, J. H. Weaver, P. Perfetti, A. D. Katnani, and G. Margaritondo, Solid State Commun. **47**, 427 (1983).
[12]A. Franciosi, P. Perfetti, A. D. Katnani, J. H. Weaver, and G. Margaritondo, Phys. Rev. B **29**, 5611 (1984).
[13]J. Nogami, C. Carbone, D. J. Friedman, and I. Lindau, Phys. Rev. B **33**, 864 (1986).
[14]J. H. Weaver, M. Grioni, J. J. Joyce, and M. del Giudice, Phys. Rev. B **31**, 5290 (1985).
[15]M. Grioni, J. J. Joyce, and J. H. Weaver, Phys. Rev. B **32**, 962 (1985).
[16]J. Nogami, M. D. Williams, T. Kendelewicz, I. Lindau, and W. E. Spicer, J. Vac. Sci. Technol. A **4**, 808 (1986).
[17]M. Prietsch, M. Domke, C. Laubschat, and G. Kaindl, Phys. Rev. Lett. **60**, 436 (1988).
[18]Since the SX700 monochromator at BESSY has no entrance slit, variations in the position of the stored electron beam lead to small changes of the photon energy.
[19]D. E. Eastman, T.-C. Chiang, P. Heimann, and F. J. Himpsel, Phys. Rev. Lett **15**, 656 (1980).
[20]F. Gerken, J. Phys. F **13**, 703 (1983).
[21]W. D. Schneider, C. Laubschat, and B. Reihl, Phys. Rev. B **27**, 6538 (1983).
[22]P. Chiaradia, A. D. Katnani, H. W. Sang, Jr., and R. S. Bauer, Phys. Rev. Lett. **52**, 1246 (1984).
[23]J. R. Chelikowski and M. L. Cohen, Phys. Rev. B **14**, 556 (1976).
[24]R. Ludeke, Surf. Sci. **168**, 290 (1986).
[25]J. Y.-F. Tang and J. L. Freeouf, J. Vac. Sci. Technol. B **2**, 459 (1984).
[26]H. F. Wolf, *Semiconductors* (Wiley, New York, 1971).
[27]J. R. Waldrop, Appl. Phys. Lett. **46**, 864 (1985).
[28]G. K. Wertheim, S. B. DiCenzo, and D. N. E. Buchanan, Phys. Rev. B **33**, 5384 (1986).
[29]G. Kaindl, T. C. Chiang, D. E. Eastman, and F. J. Himpsel, Phys. Rev. Lett. **45**, 1808 (1980).
[30]J. Kanski, S. P. Svensson, T. G. Andersson, and G. LeLay, Solid State Commun. **60**, 793 (1986).
[31]W. E. Spicer, I. Lindau, P. Skeath, and C. Y. Su, J. Vac. Sci. Technol. **17**, 1019 (1980).

[32]K. Stiles, A. Kahn, D. G. Kilday, and G. Margaritondo, J. Vac. Sci. Technol. B **5**, 987 (1987).
[33]R. Ludeke and G. Landgren, Phys. Rev. B **33**, 5526 (1986).
[34]F. Schäffler, G. Hughes, W. Drube, R. Ludeke, and F. J. Himpsel, Phys. Rev. B **35**, 6328 (1987).
[35]M. Prietsch, C. Laubschat, M. Domke, and G. Kaindl, Europhys. Lett. **6**, 451 (1988).
[36]See *Photoemission in Solids,* edited by M. Cardona and L. Ley (Springer-Verlag, Berlin, 1978), Vol. 1, Appendix.
[37]W. G. Moffat, *The Handbook of Binary Phase Diagrams* (General Electric Company, Schenectady, 1981).
[38]F. Hollinger, in *Handbook on the Physics and Chemistry of Rare Earths,* edited by K. A. Gschneidner and L. Eyring (North-Holland, Amsterdam, 1979), Vol. 4, p. 153ff.
[39]C. Laubschat, G. Kaindl, W. D. Schneider, B. Reihl, and N. Mårtensson, Phys. Rev. B **33**, 6675 (1986).
[40]B. Johannson, Phys. Rev. B **20**, 1315 (1979).
[41]A. R. Miedema, P. F. de Châtel, and F. R. de Boer, Physica B + C **100B**, 1 (1980).
[42]M. Prietsch, Ph.D. thesis, Freie Universitat Berlin, 1987.
[43]M. Domke, C. Laubschat, M. Prietsch, T. Mandel, G. Kaindl, and W. D. Schneider, Phys. Rev. Lett. **56**, 1287 (1986).
[44]K. Stiles and A. Kahn, Phys. Rev. Lett. **60**, 440 (1988).